AFRL-AFOSR-VA-TR-2019-0157

CyborgCell: Intracellular Delivery of Molecular and Supramolecular Ionic Circuits for CyborgTissue

Christine Luscombe
UNIVERSITY OF WASHINGTON

04/30/2019
Final Report

Air Force Research Laboratory
AF Office Of Scientific Research (AFOSR)/ RTB2
Arlington, Virginia 22203
Air Force Materiel Command

REPORT DOCUMENTATION PAGE

Form Approved
OMB No. 0704-0188

1. REPORT DATE *(DD-MM-YYYY)*	2. REPORT TYPE	3. DATES COVERED *(From - To)*
19-06-2019	Final Performance	01 Sep 2015 to 31 Aug 2018

4. TITLE AND SUBTITLE
CyborgCell: Intracellular Delivery of Molecular and Supramolecular Ionic Circuits for CyborgTissue

5a. CONTRACT NUMBER

5b. GRANT NUMBER
FA9550-15-1-0273

5c. PROGRAM ELEMENT NUMBER
61102F

6. AUTHOR(S)
Christine Luscombe

5d. PROJECT NUMBER

5e. TASK NUMBER

5f. WORK UNIT NUMBER

7. PERFORMING ORGANIZATION NAME(S) AND ADDRESS(ES)
UNIVERSITY OF WASHINGTON
4333 BROOKLYN AVE NE
SEATTLE, WA 98195-0001 US

8. PERFORMING ORGANIZATION REPORT NUMBER

9. SPONSORING/MONITORING AGENCY NAME(S) AND ADDRESS(ES)
AF Office of Scientific Research
875 N. Randolph St. Room 3112
Arlington, VA 22203

10. SPONSOR/MONITOR'S ACRONYM(S)
AFRL/AFOSR RTB2

11. SPONSOR/MONITOR'S REPORT NUMBER(S)
AFRL-AFOSR-VA-TR-2019-0157

12. DISTRIBUTION/AVAILABILITY STATEMENT
A DISTRIBUTION UNLIMITED: PB Public Release

13. SUPPLEMENTARY NOTES

14. ABSTRACT
Cells and cell systems coordinate their birth, growth, proliferation, and death through the exchange of information related to their environment, their function, and their interactions using messenger molecules that encode specific functions. The guided delivery of these molecules can allow programming these cells and systems towards the desired goal.
Molecular delivery has been developed for drugs with temporal and spatial control to increase the efficacy of the drug with respect to when the drug freely circulates in the bloodstream.1 Examples include drug vehicles for delayed release, for targeted delivery using specific antigen molecules present on the desired cell, and vehicles that fall apart when exposed to a given molecule that is overproduced in the area of interest such as reactive oxygen species (ROS) and H+ in areas with inflammation.2

15. SUBJECT TERMS
Cyborgcell, Molecular circuit, Cell communications, Cell control

16. SECURITY CLASSIFICATION OF:			17. LIMITATION OF ABSTRACT	18. NUMBER OF PAGES	19a. NAME OF RESPONSIBLE PERSON
a. REPORT	b. ABSTRACT	c. THIS PAGE			BRADSHAW, PATRICK
Unclassified	Unclassified	Unclassified	UU		

Standard Form 298 (Rev. 8/98)
Prescribed by ANSI Std. Z39.18

				19b. TELEPHONE NUMBER *(Include area code)* 703-588-8492

ASOFR Grant FA9550-15-1-0273

"CyborgCell: Intracellular Delivery of Molecular and Supramolecular Ionic Circuits for CyborgTissue"

PI: Marco Rolandi , co-PI: Adah Almutairi, Ali Khademhosseini

Date: 8/31/2018

Period Covered: 9/1/2015- 8/31/2018

Delivery of Cargo with a Bioelectronic Trigger

Cells and cell systems coordinate their birth, growth, proliferation, and death through the exchange of information related to their environment, their function, and their interactions using messenger molecules that encode specific functions. The guided delivery of these molecules can allow programming these cells and systems towards the desired goal.

Molecular delivery has been developed for drugs with temporal and spatial control to increase the efficacy of the drug with respect to when the drug freely circulates in the bloodstream.[1] Examples include drug vehicles for delayed release, for targeted delivery using specific antigen molecules present on the desired cell, and vehicles that fall apart when exposed to a given molecule that is overproduced in the area of interest such as reactive oxygen species (ROS) and H^+ in areas with inflammation.[2] These advances have greatly increased the efficacy and reduced the side-effects of many treatments. These advances have greatly increased the efficacy and reduced the side-effects of many treatments. Temporal control in biologically relevant timescales (ms) and single cell spatial control (10 μm) are important and can be achieved designing vehicles that respond to an external trigger.[3-4].

Bioelectronic devices and electroceuticals are able to deliver electronic and ionic impulses in the sub ms range with nanoscale spatial control to interface with biological systems. [5-6] Platforms built with biological and organic polymers with ionic and mixed conductivity are able to record and stimulate physiological functions with the delivery of ions and neurotransmitters. [7-8] Organic electrochemical transistors and transient electronics were used to record brain activity[9] and reduce inflammation.[10] Silicon nanowire field-effect transistors were used to stimulate and record cell activity from inside individual cells[11]. Bioprotonic devices have demonstrated the control H^+ currents including bioprotonic complementary transistors, diodes, synaptic memories, and transducers. [12-16] Bioelectronic devices and electroceuticals provide temporal and spatial control for electronic or ionic signals and small charged molecules.[17] Here, we demonstrate proof-of-concept delivery of a generalizable chemical messenger with triggered by a bioelectronic signal (**Figure 1**). The bioelectronic signal is provided by bioelectronic pH modulator, which triggers the falling apart of acid sensitive particles (Figure 1B). These particles contain fluorescein acetate that transforms into fluorescein upon entering neighboring cells (Figure 1C).

The bioprotonic pH modulator consists of a Polydimethylsiloxane (PDMS) well with a working electrode (WE) made of Pd/PdH, a reference electrode (RE), and a counter electrode, both Ag/AgCl. A well made of PDMS creates a channel that contains the cell culture medium to afford culturing cells on the pH modulator. The Pd/PdH WE transfers H^+ across the contact/solution interface upon an applied voltage (V). For a negative voltage applied to the WE, H^+ is reduced to H at the surface of the WE and H is absorbed onto the Pd surface to form PdH. As a consequence of this reduction and physisorption, an H^+ effectively transfers from the solution into the Pd/PdH WE thus reducing the concentration of H^+ in the solution and increasing the pH. For a positive voltage applied to the WE, the reverse occurs with an effective transfer of H^+ from

the PdH into the solution thus increasing the concentration of H^+ and consequently decreasing the pH of the solution.[16, 18-19] With this strategy, we have already demonstrated pH-induced control of bioluminescence intensity. [16, 18-19] Here, we have improved the pH control to allow pH modulation in buffer conditions, which are physiologically relevant. This is done by increasing the capacitance of the WE to afford pH control in buffered solutions, we electrochemically deposited 70 nm Pd nanoparticles (Pd NPs) on the planar Pd working electrode.[20] (Figure SI 1).

To modulate the pH in buffer condition with the pH modulator, we filled the PDMS well with 100µl standard buffered solution (1x PBS, pH= 6.0 and pH= 7.4) (**Figure 2a**). We then applied a potential difference of V= -1.0 V between WE and the RE for 20 seconds to load the Pd NPs with H^+. This process increases the pH of the buffer solution. We repeated the process three times in a fresh PBS in order to saturate the Pd NPs with H^+. We measured a negative current of i_{H+}= -2.56 × 10^{-3} A after the first 20s (Figure SI 2b, blue trace). From the measured $i_{H+,}$ we calculated the pH (Figure SI 2), which increased from pH= 6.0 to pH= 7.65 (Figure 2b, black trace, left). The calculated pH changes are in agreement with pH changes measured with a micro pH meter. We then replaced the solution with the fresh PBS 1x, pH= 6.0. In the other two rounds, we measured an i_{H+}= -0.53 × 10^{-3} A and i_{H+}= -0.47 × 10^{-3} A respectively (Figure SI 2b, blue trace). Since the change in i_{H+} for the second and third round was smaller as compared to the first one, we assumed the Pd NPs are saturated with H^+. Then we added 100 µl fresh PBS 1x, pH= 7.4 and we applied V= + 0.1V vs RE for 40 seconds and we measured i_{H+}= 3.47 × 10^{-3} A (Figure SI 2b, blue trace). The positive i_{H+} corresponds to the transfer of H^+ from the Pd NPs contact into the buffer solution. The calculated pH changed from 7.4 to 6.0 after ~ 6 seconds and stayed constant during the application of the bias for 40 sec (Figure 2b, black trace, right). We gently pipette the solution while we applied a potential difference of V= -1.0 V to homogenise

the pH change in the solution. We next integrated acid-sensitive Ac-Dex microparticles (MPs) into our bioprotonic pH modulator to study how MPs fall apart in acidic condition induced by bioelectronics signal and release the FDA into the solution.

As carriers of the chemical messenger, we used MPs that fall apart in acidic conditions when the ketal group in Ac-Dex is hydrolyzed to a hydroxyl group converting it to the hydrophilic dextran (Figure 3a).[21-23] The Ac-Dex polymer was synthesized by following the method previously described.[24] Briefly, dextran (9-11 kDa) reacts with 2-methoxypropene to obtain 66% cyclized Ac-Dex. The synthesized polymer formed into MPs by electrospray.[25] We loaded FDA into the Ac-Dex MPs by adding 10 wt% of FDA against the polymer in organic solution during particle formulation, and as a result, 1 wt % of FDA loaded into the MPs. FDA is inactive in the MPs, but it has strong fluorescence intensity (FI) after it is released and hydrolyzed.[26] Formed MPs were characterized by a fluorescence microscope. The size of the Ac-Dex MPs based on microscopy images is ca. 2.12 μm (± 0.41) (Figure SI 3a and 3b).

We integrated the MPs with the bioprotonic pH modulator to trigger they're falling apart with bioelectronic signal. We first saturated the Pd NPs with H^+ as described in **Figure 2**. We then added 100 μl of 500 μg/mL MPs in PBS 1x, pH= 7.4. We applied V= +0.1V to the working electrode vs. the reference electrode for 40 seconds to bring the pH of the solution to 6.0. We subsequently collected the samples with the MPs and stored them in dark conditions. Acidic conditions trigger the MPs falling apart by hydrolyzing the ketal group to hydroxyl group and therefore releasing FDA. We then separated the supernatant containing released FDA with a centrifuge and manually hydrolyzed FDA to fluorescein by addition of 1:1 0.2mM NaOH. We quantified the release of FDA for triggered MPs via bioelectronic pH modulator (Figure 3b, red

dots and Figure SI 4) and non-triggered MPs (Figure 3b, black dots and Figure SI 4) by using fluorometer. We measured FI, and we converted the FI to the corresponding fluorescein concentration using a calibration curve (Figure SI 4).

With the pH change triggered by the bioelectronic pH modulator, the released FDA reaches a maximum concentration (~ 2.4 μg/ ml) after 6 hrs. The FI measurements using a fluorometer were in agreement with the FI measurements using microscopy images characterization (Figure SI 6). As control, we incubated Ac-Dex MPs in phosphate buffer at pH= 6.0 and measured a smaller (1.1 μg/ml) and slower (24 hrs) release (Figure SI 5). The ketal group hydrolyzes to hydroxyl faster in lower pH or higher temperature. [27] Due to charge accumulation at the contact interface, the pH of the device/ solution interface (pH ~ 4-5) is lower than the bulk pH (pH ~6). As expected, this lower pH increases the MP degradation rate. We also monitored the MPs morphology using SEM characterization (Figure 3c). The non-triggered MPs (Figure 3c, left) have a spherical shape while the triggered MPs have a deformed shape (Figure 3c, right). Both the change in the morphology of the MPs and the FI measurements affirm that MPs successfully fall apart at pH = 6.0 compelled by bioelectronics signal and release FDA into the solution.

We next explored the delivery of FDA after Ac-Dex MPs were triggered via bioelectronic signal. To do this, we first investigated the optimum condition (MPs concentration and optimised pH) in which cells had the highest viability (Figure SI 7, a,i and b,i). We then integrated CFs into our setup to investigate the delivery of FDA after Ac-Dex MPs were triggered via bioelectronics signal (**Figure 4a**). The CFs were seeded on the bioprotonic pH modulator coated with fibronectin. After 48 hrs, LIVE/DEAD assay showed around 40% viability of the cells (Figure SI 8). We then added a medium containing 500 μg/ml Ac-Dex MPs to the cell to assess the FDA

release (Figure SI 9). We first assessed the delivery of FDA into the cells with manual pH stimulation by adding adequate amount of 0.1M HCl into the medium. By bringing the pH to 6.0 with 500 μg/ml of MPs we measured the percentage of released FDA within the cells (Figure SI 9). The uptake of released FDA into the CFs after 1hr with the manual pH stimulation was 22% at pH= 6.0 while it was negligible at pH= 7.4. (Figure SI 9).

In the presence of CFs on the bioprotonic pH modulator, we first saturated the Pd NPs with H^+ as described in Figures 2 and 3. We then replaced the solution with a fresh media containing MPs (500 μg/ml) and subsequently decreased pH upon transferring the H^+ to the solution with positive voltage of V= +0.1 V vs. RE for 40 seconds (Figure SI 11). Our bioprotonic device is stable in modulating the pH under physiological conditions (37^{o}C, physiological fluids) as it has fair reproducibility (Figure SI 12). Cells were then monitored by the fluorescent microscopy 1 hr after bioelectronic pH stimulation. To assess the amount of the uptake FDA into the cells, FI were analysed using ImageJ. The uptake of released FDA into the CFs after 1hr was 66%, which was visualized by the green fluorescence within the cells in the microscopy images (Figure 4b and 4c). Futher improvements in the kinetics of delviery are needed because incubation at pH=6 in one hour is non practical in clinical applications considering diffusion and difficulties in holding a constant pH in a biological system. For non-triggered MPs, the uptake of the released FDA into CFs after 1hr was only 3.7% and no green fluorescence observed within the cells (Figure 4b and 4d). We noticed that the cell morphology looks different with altered conditions (pH= 6.0) compared to the control (pH= 7.4) (Figure 4 c , d and SI 10). The size of the cells decreased and they became round in low pH conditions, while the cells at pH=7.4 remain flat with triangle shapes. In low-pH conditions, the cells tend to minimize the surface-to-volume (S/V) ratios because acidic environment activates inflammatory programs in cells *via* a cAMP–MAPK pathway.[28] However, the majority of the cells in both conditions were attached to the surface and thus are alive Figure SI 10). We also examined if

the applied voltage results any electroporation, which creates pores on the cell membrane and as a result helps the uptake of FDA. Microscopy images did not show the uptake of FDA within the cells under electric field without triggering the MPs. This confirms that the uptake of FDA within the cells occurs only when the MPs are triggered at pH= 6.0 and not due to the electroporation (Figure SI 13). Furthermore, the number of cells was counted before and after bioelectronic stimulation to monitor the effects of applied voltage on cell viability and data showed no significant changes in cell viability (Figure SI 14).

In this work, we demonstrated the delivery of a chemical messenger triggered by a bioelectronic signal in form of pH modulation. We showed that bioprotonic pH stimulation by modulating the pH in a buffer solution ($\Delta pH \cong 1$) provides delivery of FDA to cardiac fibroblasts. This proof-of-concept may provide an avenue for integrating bioelectronics and electroceuticals with cell functions, and expands the control capabilities of bioelectronic devices that currently include electrons, ions, and small charged molecules.

Figures

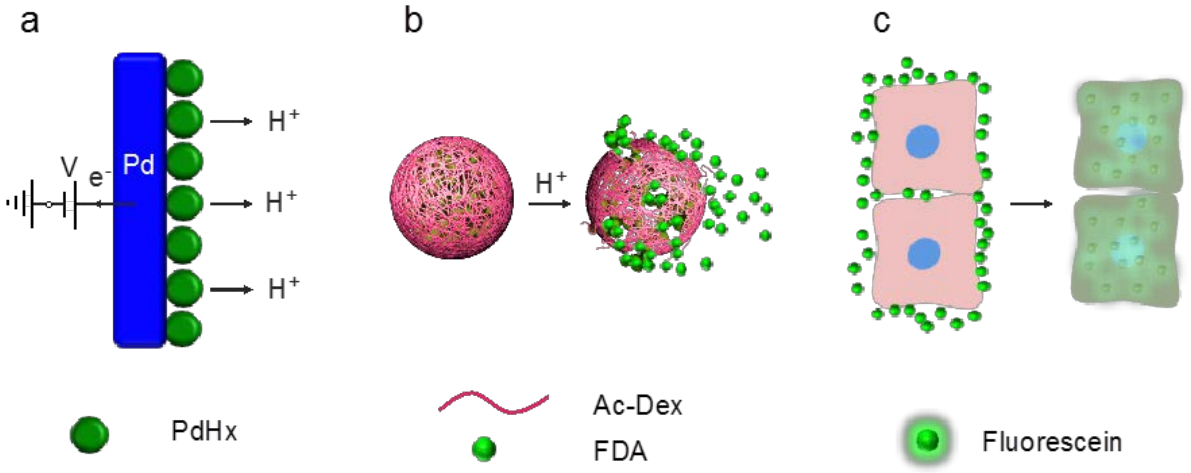

Figure 1. Schematic of the bioelectronic pH stimulation for chemical messenger delivery (a) A bioprotonic pH modulator coated with Pd nanoparticles (NPs) lowers the pH of the buffer solution upon application of a positive voltage (+V) to the Pd contact. (b) In induced acidic conditions, the acetalated-dextran (Ac-Dex) microparticles (MPs) that encapsulate fluorescein diacetate (FDA), hydrolyze to dextran and release FDA into the solution. FDA is not fluorescent before cellular update. (c) Uptake of released FDA. Upon uptake of FDA into cardiac fibroblasts, the enzyme esterase hydrolizes FDA into fluorescein, which is fluorescent. Fluorescence indicates successful delivery upon bioelectronic trigger.

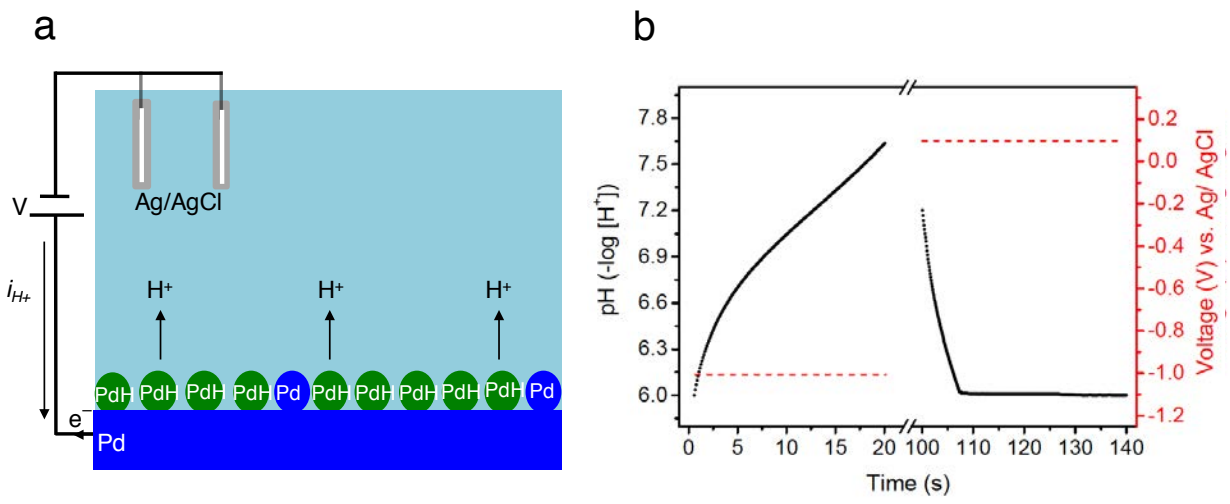

Figure 2. Bioelectronic pH modulation (a) Schematic of a bioprotonic pH modulator that changes the pH of a buffer solution upon an applied voltage (+V). (b) pH (black traces) versus time plot for V= -1.0 V and V= +0.1V (red traces). First, the protons are stored into the Pd NPs upon application of V= -1.0 V vs. Ag/AgCl for 20s, when the protons reach the surface of the Pd NPs, they get reduced to H and diffuse into the Pd. We repeated this step 3 times to saturate the Pd NPs with H^+. Second, H gets oxidized to H^+ upon application of V= +0.1V vs. Ag/ AgCl for 40s and decreases the pH to 6.0.

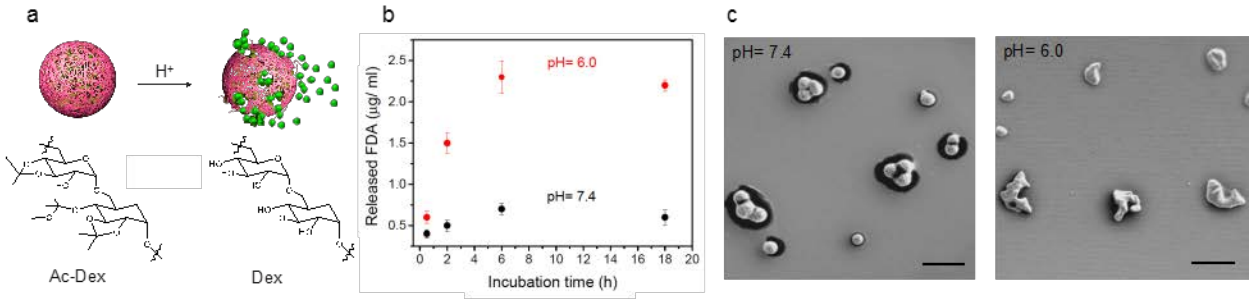

Figure 3. FDA Release by bioelectronic pH stimulation. (a) The illustration shows acid sensitive MPs that release FDA from Ac-Dex MP upon hydrolysis of Ac-Dex polymer to Dex (left, top) with the chemical structure of Ac-Dex and Dex (left bottom). (b) Released FDA versus incubation time showing the degradation of MPs after a bioelectronic pH stimulation, pH= 6.0, (red trace) and with no bioelectronic pH stimulation, pH= 7.4, (black trace). At each time point, released FDA was separated from MPs by centrifugation. The emission was measured upon addition of 1:1 0.2 mM NaOH: supernatant ratio to activate FDA to fluorescein. The FI then becomes converted to FDA release using the calibration curve of the known fluorescein solutions (Figure SI 5). (c) SEM images of the non-triggered MPs (pH= 7.4) (left) and triggered MPs (pH= 6.0) (right). 2 µl of particle solution after removing the salts was put on a silicon wafer for SEM imaging. The scale bar in SEM images is 5 µm.

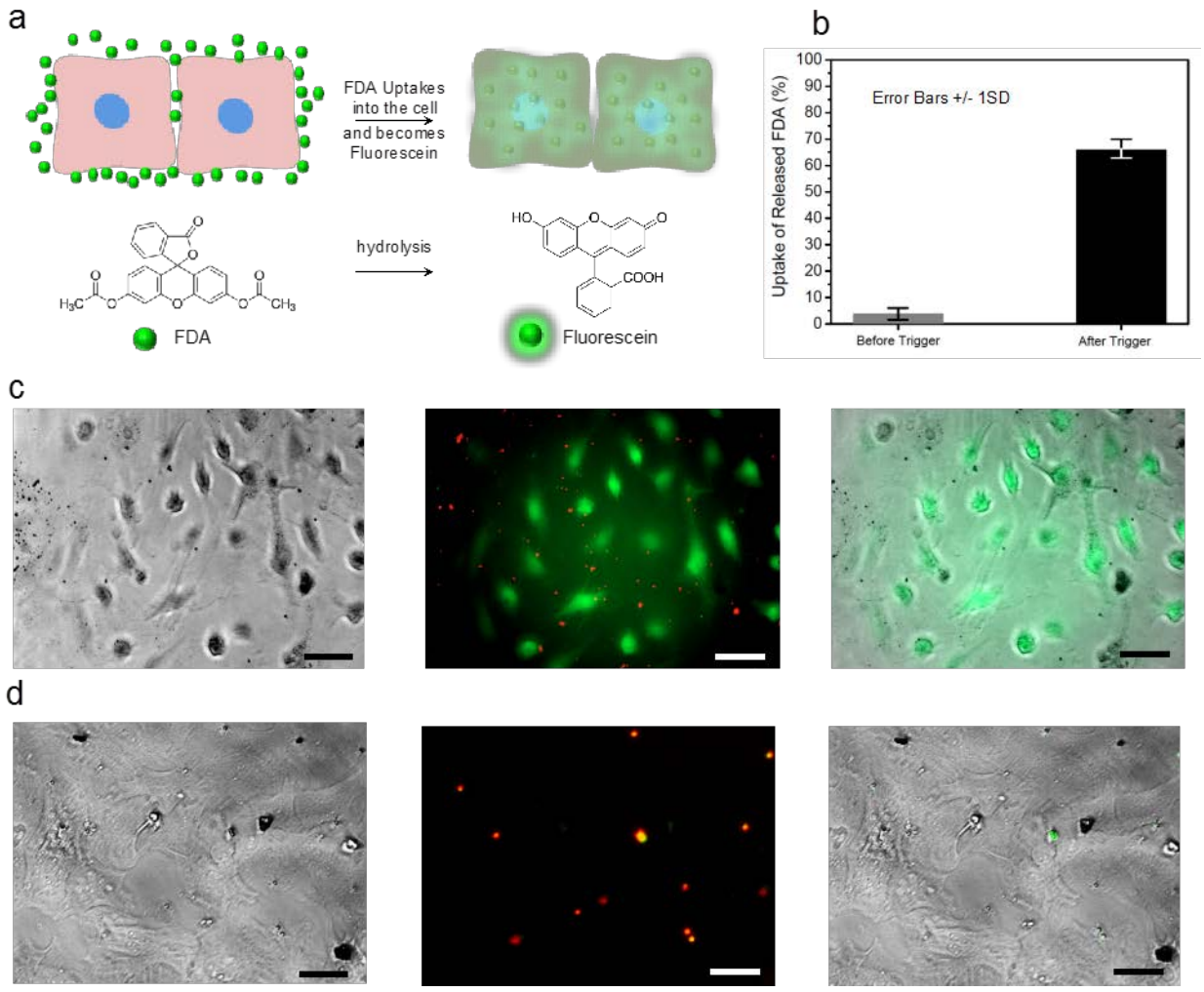

Figure 4. Uptake of Released FDA. (a) Schematic shows the uptake of the released FDA by the cardiac fibroblasts (top) and the chemical structure of FDA hydrolysis into fluorescein. (b) The uptake of released FDA before bioelectronic trigger (FDA expressed in 3.7% of cells) and 1 hour after the bioelectronic trigger (FDA expressed in 66% of the cells). The Fluorescein release is calculated from n = 10 fluorescence images (c) Fluorescence images of the cardiac fibroblasts captured 1 hr after bioelectronic trigger. Bright field image (left) and Rho-MPs/ FITC image of the cells show the uptake of FDA into the cell and hydrolysis to fluorescein as the cells have green fluorescence brightness. Bright field overlay with FITC image of the cells (right). (d) Fluorescence images of the cardiac fibroblasts captured before bioelectronic trigger.

EXPERIMENTAL SECTION.

Bioprotonic pH modulator: The protonic devices are fabricated on microscope glass slide (2.5cm x 4.5cm VWR). 100 nm Pd with a 15 nm Cr adhesion layer in the area of 12 mm2 is deposited via e-beam evaporation (Balzers PLS 500). The Pd surface is coated with a layer of Pd nanoparticles (PdNPs) via electrochemical deposition. Polydimethylsiloxane (PDMS) wells are used as solution containers and attached to the Pd substrates with PDMS. For the pH modulation in the physiological condition Ag/AgCl pellet electrodes are used as a Counter Electrode (CE), Ag/AgCl glass electrode is used as Reference Electrode (RE) and Pd/ Pd NPs contact are used as Working Electrode (WE). Electrochemical measurements are performed with a potentiostat from Metrohm.[1]

Electrical measurements: All electrical measurements were performed using Potentiostat PGSTAT128N with FRA32M Module from Metrohm.

Microscope images: The Fluorescence images of the MPs were collected using a BZ-series fluorescence microscopy of BZ-X710 from Keyence.

Scanning Electron Microscopy (SEM): SEM measurements were performed by a Quanta 3D FEG of Secondary electron detection (standard SEM) in Dual-Beam Microscope User Facility at UCSC. Before doing the SEM measurements, the samples were coated with 5nm of Au. By using a precise view of the surface of Pd contact following the Au deposition, based on the optimal duration for the electrodeposition of PdNPs we could determine the number and spacing

of individual PdNPs. We also determined the shape of the MPs before and after degradation using SEM characterization.

Fluorescence measurements: All the fluorescence intensity (FI) measurements were performed by a fluorometer from Horiba scientific Model FluoroMax-3.

Synthesis of pH-sensitive AcDex Microparticles (MPs): pH-sensitive acetalated dextran (Ac-Dex) was synthesized by following and modifying a previously described method. Dextran (10 – 12 kDa, from *Leuconostoc mesenteroides*), 3 g (18.5 mmol), was dissolved in 27 ml of anhydrous dimethyl sulfoxide (DMSO) and followed by addition of *p*-toluenesulfonic acid (18 mg, 71.6 mmol). After 15 min, 2-methoxypropene (10.2 ml, 106.37 mmol) was slowly added into the solution and stirred at room temperature. After 3 hrs, the reaction was quenched with 5 mL triethylamine. The newly synthesized polymer was precipitated in 0.01% trimethylamine containing water. This precipitation process was repeated three times to further purify the polymer. The product was a white solid (3.34 g, 84 % yield). Rhodamine conjugated Ac-Dex was also prepared for particle tracking. It was synthesized with same method by acetalizing rhodamine conjugated dextran (10 kDa). pH sensitivity is affected by the ratio of cylcic to acyclic acetal groups. To calculate cyclic ratio of the resulting Ac-Dex, the suspension of Ac-Dex in D_2O was added a small amount of deuterium chloride (1 % DCl). The cyclic ratio was calculated by comparing proton NMR peaks of acetone and methanol. [2] As a result, cyclic ratio of acetalated polymer (Ac-Dex) was 66 %.

Microparticle formulation: Ac-Dex, 60 mg, and 6 mg of Lutrol F 126 were dissolved in 80 µl of DMSO and 320 µl of CHCl3. The polymer solution was injected into a capillary tube with a flow rate of 0.18 ml/min. A voltage of ~ 16 kV was applied and the particles were collected onto

slides. Sprayed particles were dried for overnight in a desiccator. Dried particles were re-dissolved in PBS and washed 3 times by centrifuge (4500 rpm, 10 min, 20 ^{o}C).

pH-triggered MPs deformation: 0.1 mg/mL Ac-Dex MPs in pH= 6.0 and pH= 7.4 phosphate buffer were incubated at 37 ^{o}C for 2 days. The incubated MPs are diluted with H_2O and put on a silicon wafer. After drying overnight under vacuum, the MPs are coated by a sputter coater and observed by SEM.

pH-triggered cargo release from MPs: 1 mg of FDA loaded Ac-Dex MPs were dissolved in 10 mL of pH 6.0 and pH 7.4 phosphate buffer. The MPs solutions are incubated at 37 ^{o}C and released FDA was separated from MPs by centrifugation (13000 rpm, 10 min, 20 ^{o}C) at each time point. The collected FDA was hydrolyzed by 1 M NaOH and emission was measured by fluorometer (Figure SI 5).

Fibroblast cell culture: In order to verify the delivery of pH-sensitive FDA-loaded Rho-AC-Dex particles into the cells and evaluate the release of FDA into the cells, cardiac fibroblasts (CFs) were isolated from 1 to 2 day old neonatal Sprague Dawley rats using a protocol approved by the Institute's Committee on Animal Care [3] and were used as cells of interest.[4] Cells were cultivated in DMEM-high glucose medium (Gibco-11965-092) supplemented with 10 % FBS (Gibco, 10437-028), 1 % L- Glutamine (Gibco, 25030-081), 1 % penicillin/streptomycin. Cardiac fibroblasts were used between passages 2-5. Each Pd NP protonic device were washed with several times with 70 % ethanol and coated with 10 % fibronectin for 1hr in room temperature. Cells were seeded at the density of 1.6×10^5 cells/cm^2 and left for 48 hrs to settle. Then, Rho-AC-Dex particles were added in the same medium and at the concentration of 0.5 mg/ml. Then MPs were sonicated in a water sonicator bath for 5 min and then were centrifuged at 3000 rpm

for 15 min at 20 ^{o}C. Supernatant were removed and MPs re-suspended in medium and washing step repeated one more time. Then cardiac fibroblasts were incubated with MPs dispersed medium for 1 hr. To make pH 6.0 culture condition for particles to release FDA, appropriate amount of 0.1M HCL were added to the medium containing MPs (previously optimized) soon after adding the MPs to the cells. In the case of bioelectronic pH stimulation, media solution containing MPs in neutral pH (7.4) was added to the cells seeded on Pd/ Pd NPs contact and the flow of H^+ from the contact to the solution provides upon application of V = 0.3 V vs. Ag/AgCl for 40 sec. After 1 hr cells were washed with medium for few minutes to and cells were assessed for FDA-release using fluorescent microscopy.

Microscope images: All microscope images were performed using fluorescence microscope (Axio Observer D1, Carl Zeiss) and Image J software was used for analysis.

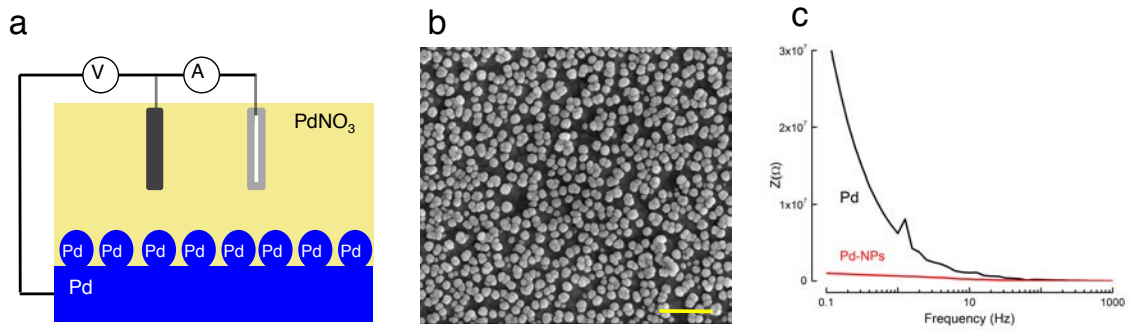

Figure SI 1. (a) The scheme of electrochemical deposition of Pd NPs to improve H^+ transport in buffer condition. Planar Pd is used as working electrode (WE), Ag/AgCl as a reference electrode (RE) and Pd wire as a counter electrode (CE). We added 100 □g/ml PdNO3 solution into the PDMS well and we applied a potential difference of V= -0.8V between Pd and RE for 100 sec to deposit Pd NPs. (b) SEM images of the Pd NPs deposited on the planar Pd contact. The scale bar is 500nm. The NPs has the size of ca. 70 nm (± 5). (c) Electrochemical impedance spectroscopy (Bode plot) shows the impedance of a planar Pd contact (black trace) and planar Pd contact coated with Pd NPs in a PBS 1x pH= 7.4. Pd contact is used as a WE and Ag/AgCl electrodes is used as a RE and CE. The impedance as a function of frequency plot was recorded when a10mV AC signal was applied at frequencies ranging from 0.1Hz to 100kHz. It shows that the Pd planar contact coated with Pd NPs exhibits lower impedance than planar Pd contact. It is inversely proportional to the higher capacitance of the Pd contact coated with Pd NPs compare to planar Pd contact.

To calculate the surface area of the Pd contact coated with Pd NPs we first calculate the surface area of single NPs according to the size of the NPs ca. 70nm (± 5) measured by SEM, Area of

Circle (A_C) $A_C = \Pi r^2$, where $\Pi = 3.14$ and r is the radius. Considering the surface area of the planar Pd contact ca. 12 mm^2 and the surface area of a single Pd NPs ca. 3.85×10^{-9} mm^2 we estimate the number of Pd NPs coated the surface ~ 3×10^9. Because the NPs have the spherical shape we then calculate the surface area of Pd NPs ca. 46 mm^2, with Area of Spherical (A_S), $A_S = 4\ \Pi r^2$, and considering the estimated number of Pd NPs. Since the spacing between Pd NPs collected by SEM images is the same as the size of Pd NPs, therefore the final surface area of the Pd contact coated with Pd NPs is 52 mm^2. Comparing the surface area of the planar Pd ca. 12 mm^2 the surface area of the Pd contact coated with Pd NPs is ~ 4 times higher that planar Pd contact.

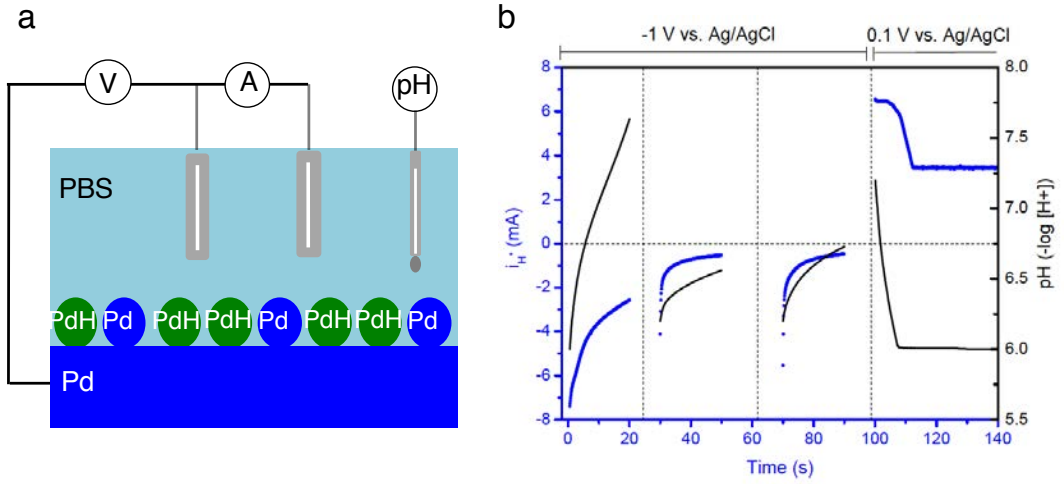

Figure SI 2. (a) The scheme of the Pd contact device coated with Pd NPs that provides the transport of H^+ from/ to Pd NPs contact upon application of voltage (V). (b) The proton current (i_{H+}) vs time graph (blue trace) and the calculated pH vs time graph (black trace). The PDMS well was filled with 100□l PBS 1x, pH=6.0. We applied V= -1.0 V vs. RE for 20sec. The proton current changed from $i_{H+} = -7.40 \times 10^{-3}$ A to $i_{H+} = -2.56 \times 10^{-3}$ A (black trace). From the total charge collected to the leads we calculated the pH changes (Note SI

1) for the first 20 sec. The pH changed from pH= 6.0 to pH= 7.8 (black trace). We then replaced the solution with a fresh PBS 1x, pH= 6.0 and we applied V= -1.0 V vs RE for the second 20 sec. The proton current changed from i_{H+}= -4.11 × 10^{-3} A to i_{H+}= -0.53 × 10^{-3} A (blue trace). Which correspond to the change of pH from pH= 6.2 to pH= 6.55 (black trace). We again replaced the solution with fresh PBS 1x, pH= 6.0 and we applied V= -1.0 V vs RE for the third 20 sec. The proton current changed from i_{H+}= -5.53 × 10^{-3} A to i_{H+}= -0.47 × 10^{-3} A (blue trace). Which correspond to the change of pH from pH= 6.2 to pH= 6.7 (black trace). To transport the H+ to the solution and bring it to acidic condition, we then replaced the solution with the fresh PBS 1x, pH= 7.4 and we applied V= +0.1V vs RE for 40sec. The proton current changed from i_{H+}= +6.75 × 10^{-3} A to i_{H+}= +3.47 × 10^{-3} A (blue trace). Which correspond to the change of pH from pH= 7.2 to pH= 6.0 (black trace).

Note SI 1

The area under the i_{H+} vs. time graph results the charge transport of H^+. We calculate the concentration of H^+, $[H^+]$, in 100 µl of buffer solution using Faraday constant, 96485.33289 C mol^{-1}. We then calculate the pH change in PBS buffer solution using the "*Henderson Hasselbalch Equation*"[5].

$$pH = pK_2 + log\frac{[HPO_4^{2-}]}{[H_2PO_4^-]} \qquad (1)$$

$$K_2 = \frac{[H^+][HPO_4^{2-}]}{[H_2PO_4^-]} \;;\; [H^+] = \frac{K_2[H_2PO_4^-]}{[HPO_4^{2-}]} \qquad (1)$$

,which can be converted to:

$$pH = pK_2 + log\frac{[HPO_4^{2-}]}{[H_2PO_4^-]} \qquad (2)$$

where pH = -log[H^+], and pK_2 = -logK_2. The latter logarithmic expression called the "*Henderson Hasselbalch Equation*" is a convenient form to use in buffer calculations, particularly when the pH is within one unit above or one unit below the pK. (Where the ratio $[HPO_4^{2-}]/[H_2PO_4^-]$ is between 0.10 and 10). Although all four species of phosphate are always present in solution, the two forms in the equation are the predominant ones near the pK and the others can usually be ignored in calculations. As one gets more than two units above or below the pK, however, other species become involved and the calculations get more complicated.

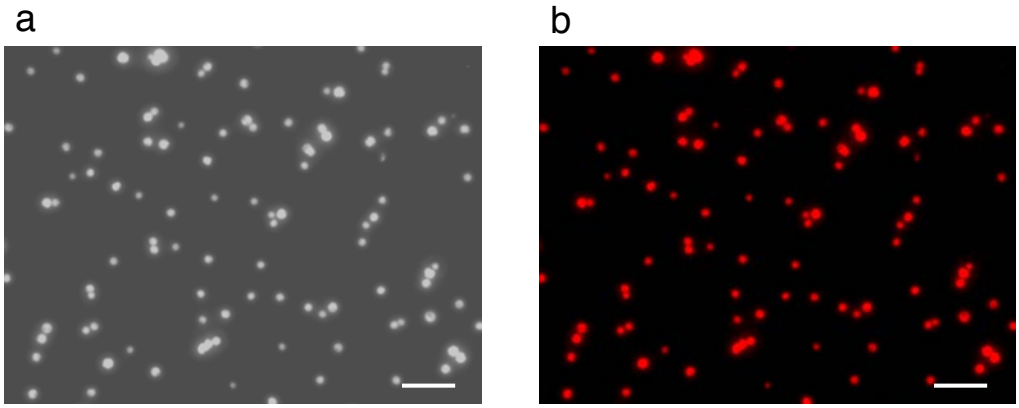

Figure SI 3. Microscopy image of MPs incubated in PBS 1x, pH= 7.4 (a) the dark field image and (b) the rhodamine fluorescence channel image evaluate that the size of MPs ca. is 2.12 ± 0.41 µm. The data are collected from 3 different Images. The red color is corresponding to conjugated rhodamine dye on the Ac-Dex polymer. The scale bare in the images is 10 µm.

Calculation of cyclic to acyclic ratio of Ac-Dex

The acetal ratio of cyclic to acyclic was calculated based on ^{1}H-NMR. Ac-De polymer (5 mg) was dispersed in 1 ml of D_2O, and DCl was added on the solution. After 5 minutes of vortex, proton peaks were evaluated by NMR spectroscopy. Since cyclic acetals resulting acetone by hydrolysis while acyclic acetals resulting methanol and acetone, integration values of the methanol peak (3.34 ppm) and acetone peak (2.08 ppm) were compared to calculate cyclic to acyclic ratio, as previously described. [2] Consequently, 66 % of acetals were cyclic.

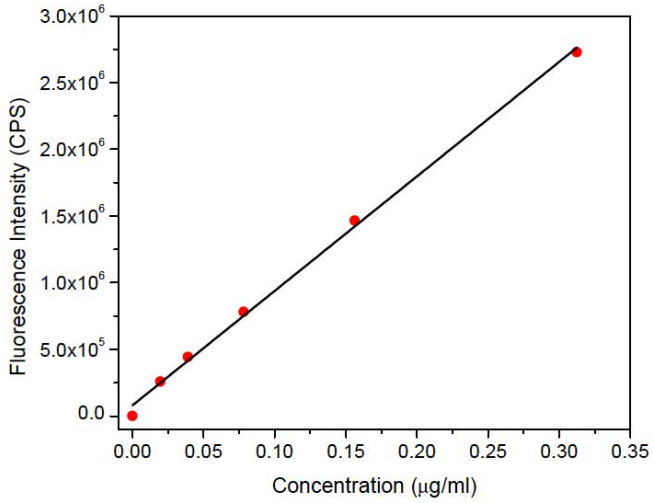

Figure SI 4. Fluorescein calibration curve for calculation of released FDA. We suspended the FDA into PBS 1x pH= 7.4 for the final concentration of 0 µg/ml, 0.02 µg/ml, 0.04 µg/ml, 0.08 µg/ml, 0.15 µg/ml and 0.30 µg/ml. For each of these samples we measured the Fluorescence intensity of the FDA solution upon addition of 1:1 0.2 mM NaOH to hydrolyze the FDA. We then plotted the Fluorescence intensity of known FDA solution vs. the corresponding concentration. We fit the experimental data with the linear fitting to obtain the calibration curve

of Y= 4 $\times 10^{+6}$ X + 34328 (R^2= 0.9981). We then used this calibration curve to calculate the released FDA from the MPs from the measured fluorescence intensity.

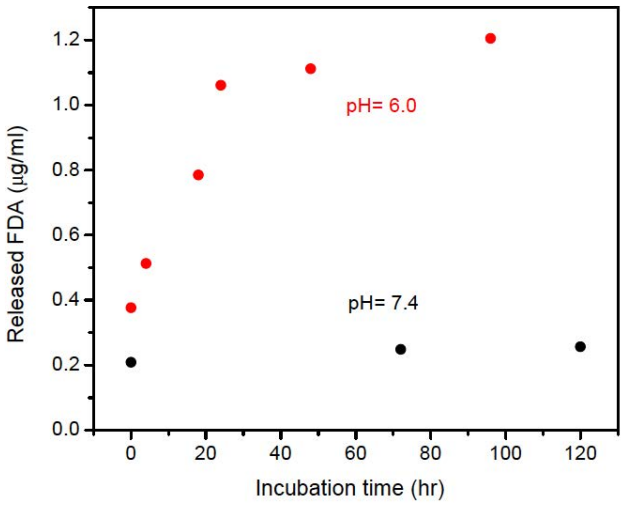

Figure SI 5. Release of FDA from Ac-Dex MPs at pH 6.0 (black) and pH 7.4 (red). We used the calibration curve (Figure SI 4) to convert the measured fluorescence intensity to the released FDA.

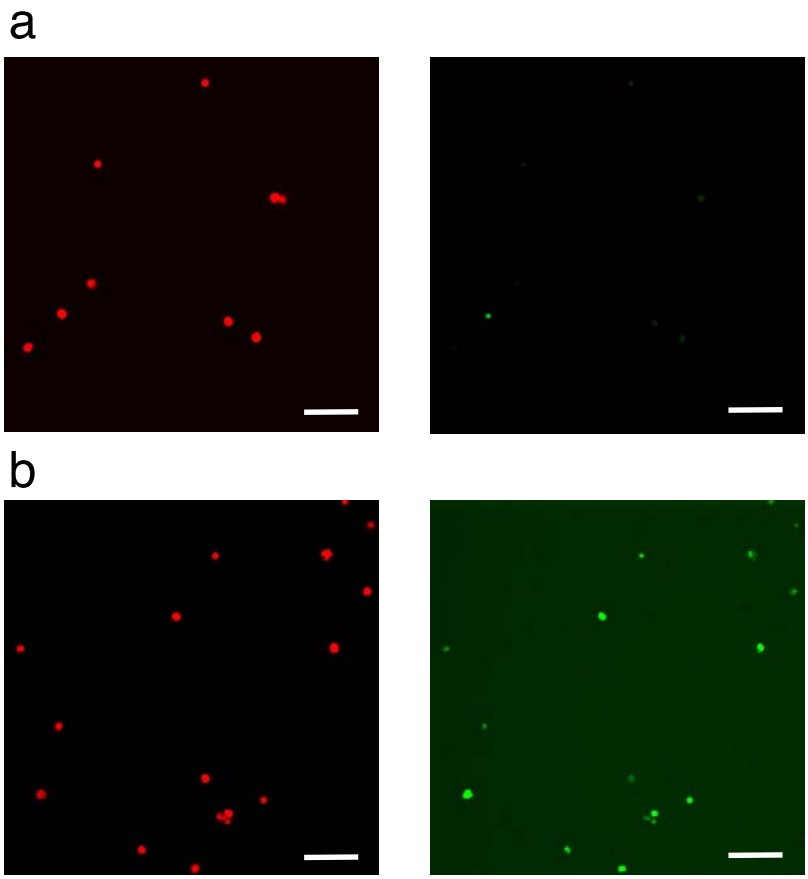

Figure SI 6. (a) The microscopy images of the MPs before bioelectronics trigger. The red color (left) is corresponding to the presence of rhodamine dye that is attached to the Ac-Dex MPs to be detectable. The size of MPs is ~ 2 μm. The green color and its corresponding fluorescence intensity (right) have very low intensity of ca. 0.07 RFU (± 0.02), which confirms that FDA is still encapsulated inside the MPs. (b) The microscopy images of the MPs after bioelectronics trigger. The red channel image (left) is the MPs 2 hrs after bioelectronics trigger. No significant change observes for the size of MPs while they were in the solution. But the green color (right) and its fluorescence intensity has high intensity of ca. 2.4 RFU (± 0.3) for MPs as well as the background solution, which confirms that FDA is released and hydrolyzed upon addition of 0.2 mM NaOH. The data is collected from 3 different images for each condition. The images are

analyzed under stack mode ROI method with equal intensity, brightness and contrast. The scale bar in images is 10 μm.

Viability test in different concentrations of pH-sensitive MPs in 3T3 cells

We investigated the optimum condition (MPs concentration and optimised pH) in which cells had the highest viability. We first investigated the pH-sensitive MPs (size: 2.12 μm (± 0.41) in three different concentrations (100, 500 and 1000 μg/ml). Prestoblue viability test illustrated significant reduction (*$P < 0.05$) in cell viability in 1000 μg/ml concentration compared to control condition. Furthermore, considerable reduction in cell density and several areas of particle aggregation was observed in 1000 μg/ml concentration using phase-contrast microscopy. However, cells in concentrations of 100 and 500 μg/ml showed similar viability and density compared to control condition. Therefore, 500 μg/ml was chosen as the optimum concentration for pH-sensitive MPs (Figure SI 7 a, b). In the next step, in order to find out the toxicity of different pH on cell viability, cells were stimulated with 500 μg/ml MPs in three different pH (5.0, 6.0 and 7.4) and compared to control condition. Control condition just contained medium in different pH condition. Prestoblue viability test showed significant reduction (*$P < 0.05$) in cell viability in pH 5 compared to pH 6 and 7.4 in both control and stimulated cells with particles. Therefore, pH 5 considered to be toxic for the cells. Thus, pH 6 and 500 μg/ml concentration was selected as the optimised condition (Figure SI 7 c, d).

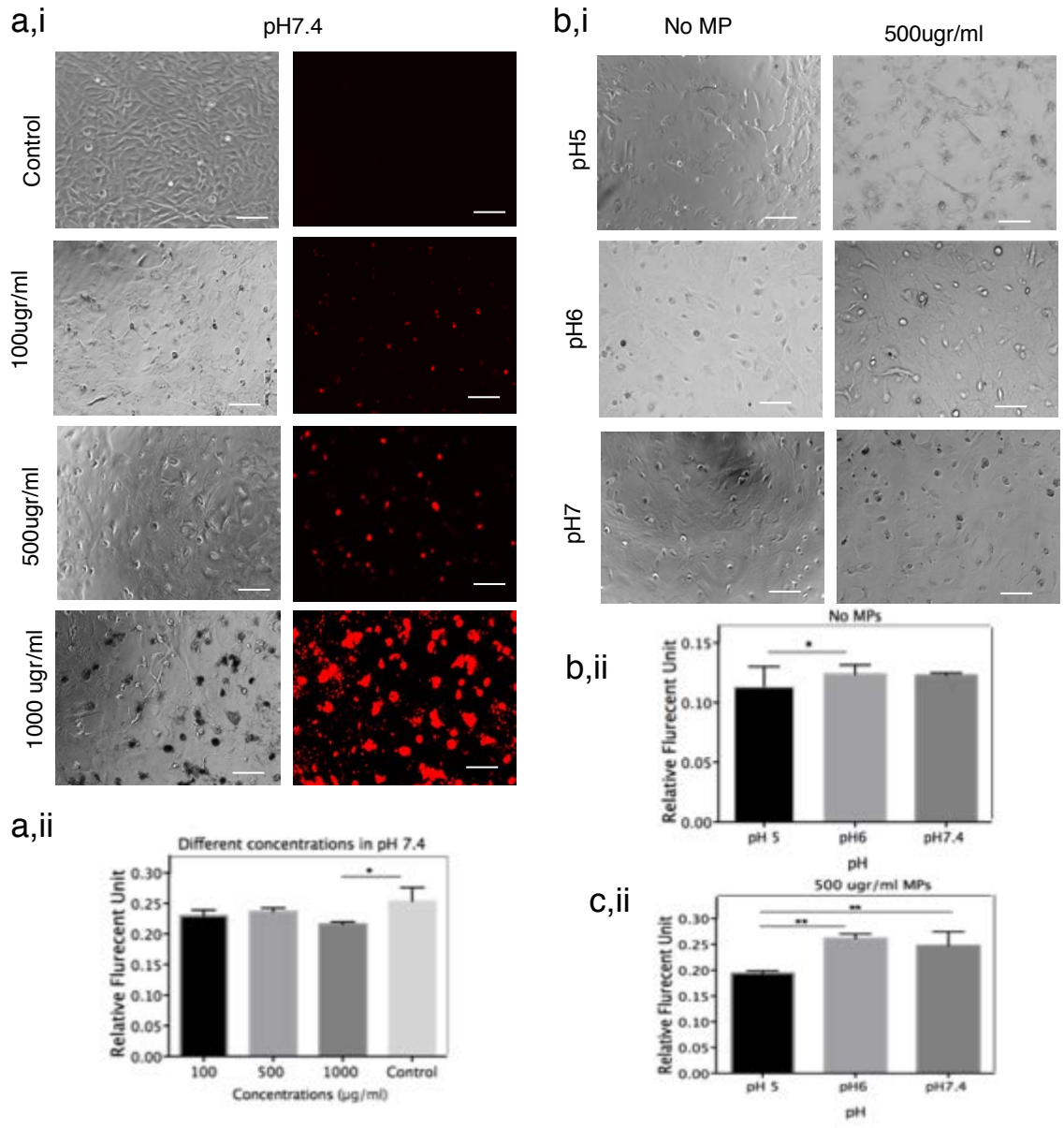

Figure SI 7. Optimization of the concentration and pH for MPs; (a) Representative images of cells in presence of MPs in different concentrations (100, 500 & 1000 µg/ml). Phase contrast microscopy were used to assess the cell morphology and density which showed big areas of cell death in 1000 µg/ml. Also, assessing Rhodamine-conjugated to particles in red channel showed increased aggregation pf particles in 1000 µg/ml. (b) Cell viability test in different concentrations of pH-sensitive MPs; Statistical analysis (using prestoblue) showed significant

reduction (*$P < 0.05$) in 1000 µg/ml concentration compared to other conditions. Scale bar 100µm (biological replicate=3 times & Technical replicate= 5 for each concentration). (c) Cells were cultured in three different pH 5, 6 7.4 (first raw). Phase contrast microscope showed remarkable reduction in cell density and morphology. (d) Cell viability test showed significant reduction (*$P < 0.05$) in cell viability. (e &f) Finally, cells were stimulated with optimum concentration of MPs 500 µg/ml in three different pH. Phase contrast microscope showed remarkable reduction in cell density which was confirmed with cell viability test. Scale bar 100µm.

Cell attachment and viability on bioelectronic trigger device

In order to find whether cells can attach to the Pd NPs surface,devices were first washed with 70% ethanol. Then they were washed 3 times with PBS + 5% Pen-Strep and then coated with fibronectin (10 µg/ml). Cells were then seeded in 1.6×10^5 cells/cm^2 in DMEM+10% FBS and left for 48 hrs to settle. Then, cells were fixed with 4% PFA and stained for F-actin and DAPI. Furthermore, cells were stained with LIVE/DEAD Cell Viability Assay to discriminate the population of live cells from dead-cell population and quantified using ImageJ. Percentage of dead cells (61 %) were approximately two times more than live cells (39 %). F-actin staining showed considerable amount of cell attachment to the surface.

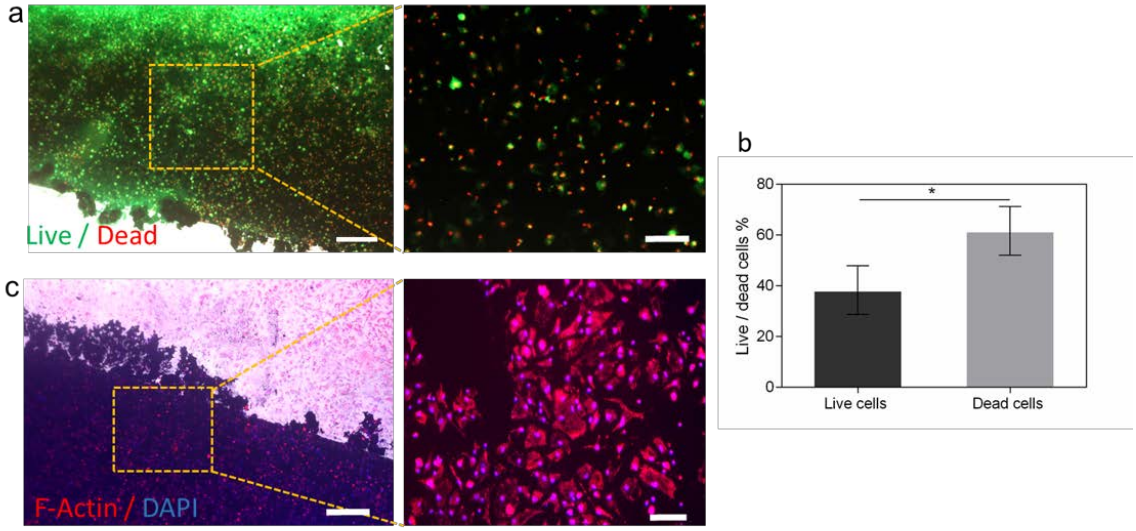

Figure SI 8: Assessment of cell attachment on Pd NPs surface. (a) LIVE/DEAD staining illustrates live cells in green and dead cells in red. (b) Quantification of live and dead cells showed significant difference (*$P < 0.005$) between live and dead cells. (c) Cells were stained for F-actin and DAPI to better observe cell attachment to the surface. Scale bar for the two left images is 500µm and for the two right images are 200µm.

Assessment of FDA uptake with manual stimulation

In order to assess the uptake of FDA with manual pH stimulation cardiac firoblast cells were seeded on fibronectin coated PdNP protonic device and left for overnight to settle. After 24 hrs, medium containing MPs were added to the cells. Then appropriate amount of 0.1M HCl were added to the media to reach the pH 6. Uptaken of FDA were assessed under the microscope at time zero, 1 hr and 6 hrs respectively. Fluorescent microscopy observations illustrated that FDA was uptaken within the cells after 1 hr and 6 hrs at pH 6 whereas no FDA was uptaken within the cells even after 6 hrs at pH 7.4. Statistical analysis showed this difference was significant. (**$P <$ 0.005).

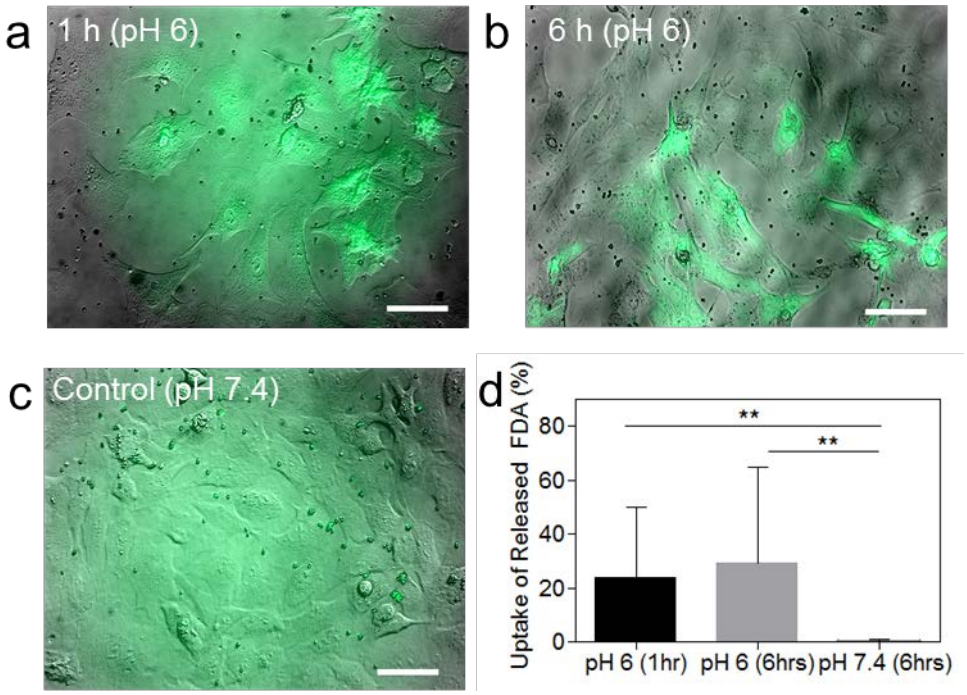

Figure SI 9. The uptake of FDA in different pH and time courses; Florescent microscopy observations showed that cells have uptaken the FDA 1hr after stimulation (a) which was also observed after 6hrs (b). No FDA up taken was observed in control condition (c). Statistical analysis further confirms the significant difference between different FDA up taken in pH 6 (both 1hr and 6 hrs) versus pH 7.4 (d). Scale bar 50μm.

Assessment of cell morphology at different pH values

In order to see the effect of acid treatment on cell morphology, cardiac fibroblast cells were seeded on 96 well-plates 2 x 10^4 cells/well on DMEM+10%FBS and were left overnight to settle. Then 0.1M HCl was used to make a media with pH 6. Next, this media was added to the cells and were left for 6 hours. Then the morphology of the cells was assessed under the bright field microscope. In low-pH conditions, the cells tend to minimize the surface-to-volume (S/V) ratios [6]. Our observations illustrated that size of the cells were decreased in pH 6.0 compared to pH 7.4 and the shape of the cells changed towards more round shape compared to flatten and triangle shape of the cardiac fibroblasts in pH 7.4. In pH 6, it was observed that some of the cells were white round-shape and were starting to detach from the surface due to the low protein attachment factors which results from cells going through the apoptosis phase. This suggests that low pH is not the optimum pH environment for the cell viability. However, majority of the cells in both conditions were attached to the surface and thus are alive. Therefore, these observations demonstrated that the morphology and the S/V ratios of cardiac fibroblasts were changed in response of the chaining pH level of the environment.

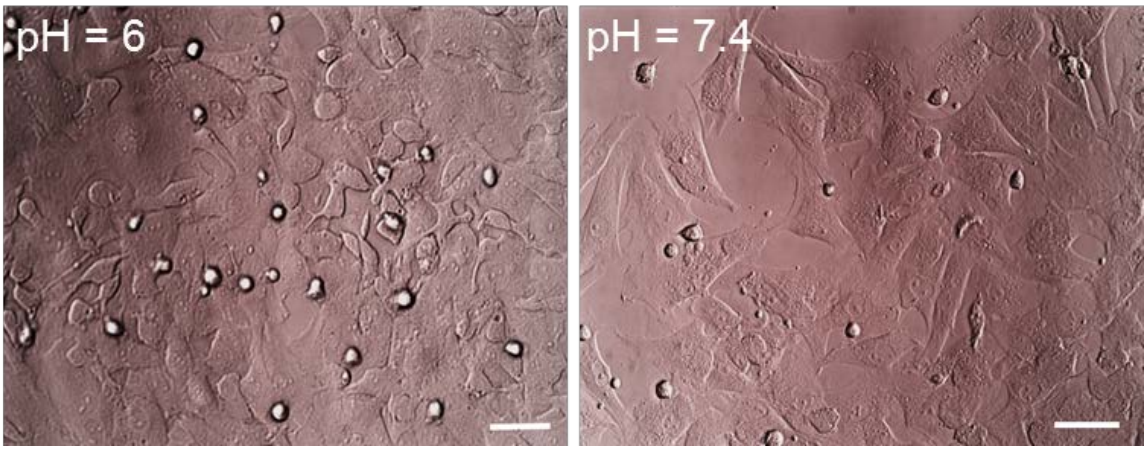

Figure SI 10. Cells morphology in pH=6.0 vs pH=7.4. Bright field images illustrated that cells size decreased in pH= 6.0 compared to pH= 7.4. Also, shapes of the cells were more round shape in pH= 6.0 compared to flatten and triangle shape in pH= 7.4. Scale bar 50µm.

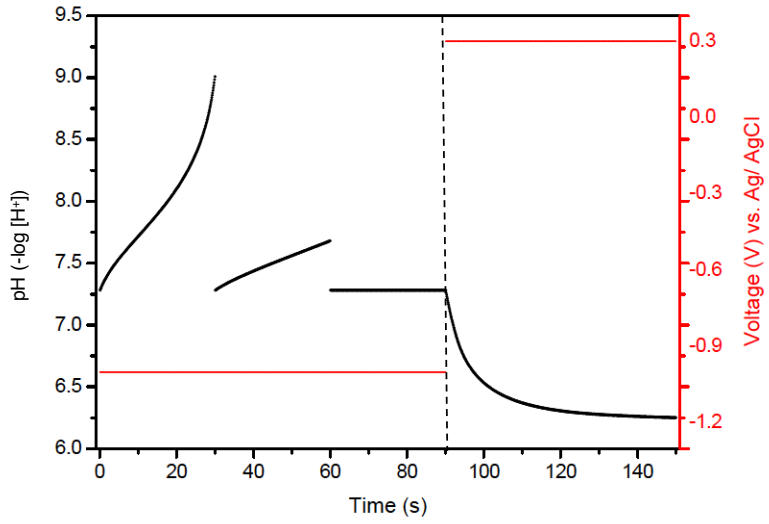

Figure SI 11: The bioelectronics triggering of MPs at the interface of cardio fibroblast. In this experiment we started with media pH= 7.4 while the fibroblast cells are already cultured on top of Pd NPs contacts. The pH changes from pH= 7.4 to pH= 9.0 upon application of V= -1.0V vs. RE for 30 sec. We replaced the solution with a fresh media pH=7.4. The pH changes from pH 7.4 to pH 7.7 upon application of V= -1.0V vs. RE for the second 30 sec. We again replaced the solution with a fresh media at pH 7.4. We did not see any significant change in the pH of the media solution upon application of V= -1.0V vs. RE for the third 30 sec. We replaced the solution with the fresh media at pH 7.4 containing 500 µg/ml MPs. Upon application of V= +0.3 V vs. RE the pH changed from pH= 7.4 to pH= 6.2. This pH change triggered the MPs and releases the FDA.

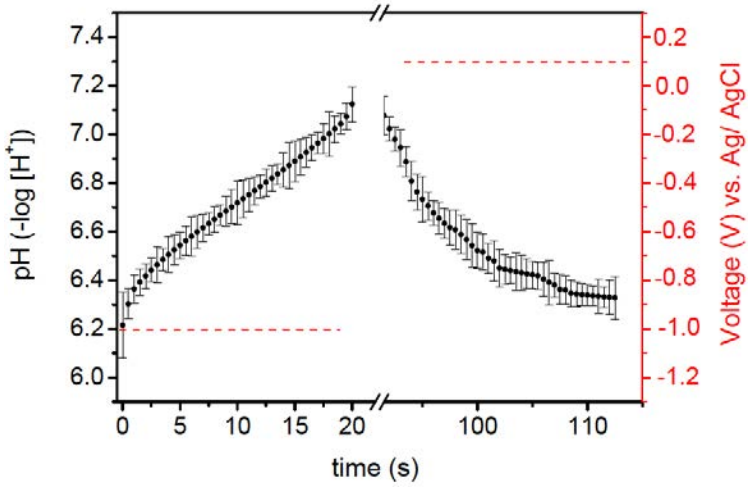

Figure SI 12: The bioelectronics triggering of MPs at the interface of cardio fibroblast. In this experiment we started with media pH= 6.2 while the fibroblast cells are already cultured on top of Pd NPs contacts. The pH changes from pH 6.2 to pH 7.1 upon application of V= -1.0V vs. RE for 20 sec. We replaced the solution with the fresh media pH 7.4 containing 500 µg/ml MPs. Upon application of V= +0.1 V vs. RE the pH changed from pH 7.4 to pH 6.2. This pH change triggered the MPs and releases the FDA. We used the same PdH electrode for several experiment (the data are collected from 3 different experiment using the same PdH electrode). The calculated standard deviation is greater than 0.035 and less than 0.099 confirming the stability of PdH electrodes upon changing the pH in several experiments.

Control experiment for FDA-released MPs using bioelectronic device

We applied a control experiment to find out whether FDA uptake within the cells was only due to the reduction of pH through the release of H^+ flows within the solution and not as a result of the electroporation which created pores on the cell membrane upon the application of electric field [7,8]. In order to perform this experiment, cells were seeded on Pd NPs and media containing MPs (pH 6) were added to the cells. Then negative voltage V=-1V vs. Ag/AgCl was applied for 20 sec and this step was repeated for three times. However, the application of positive voltage as the second part of the process was excluded to prevent the H oxidation. Then, FDA uptaken were assessed under the fluorescent microscopy after 1hr. Microscopic observation did not show any FDA uptaken within the cells which confirmed that FDA is only released and uptaken within the cells in low environmental pH and not due to the electroporation.

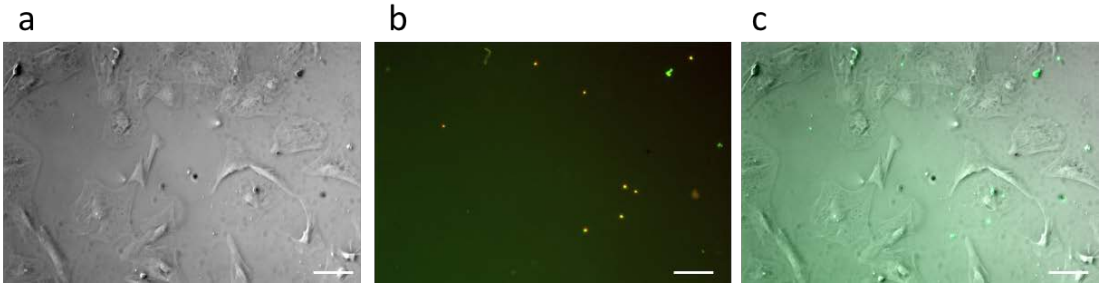

Figure SI 13: Electronic stimulation of cell membrane in presence of MPs on Pd NP device. Cardiac fibroblasts were plated on fibronectin coated Pd NPs. MPs were then added to the cells. Then cells were exposed to negative voltage (V=-1V vs. Ag/AgCl) 20 sec for three times. Fluorescence images of the cells captured 1hr after electrical stimulation. (a) Bright field image of the cells. (b) Rho-MPs + FITC image of the cells. (c) Bright field + FITC image of the cells did not show fluorescein uptake into the cells. Scale bar 100μm.

Assessment of cell number before and after electronic stimulation

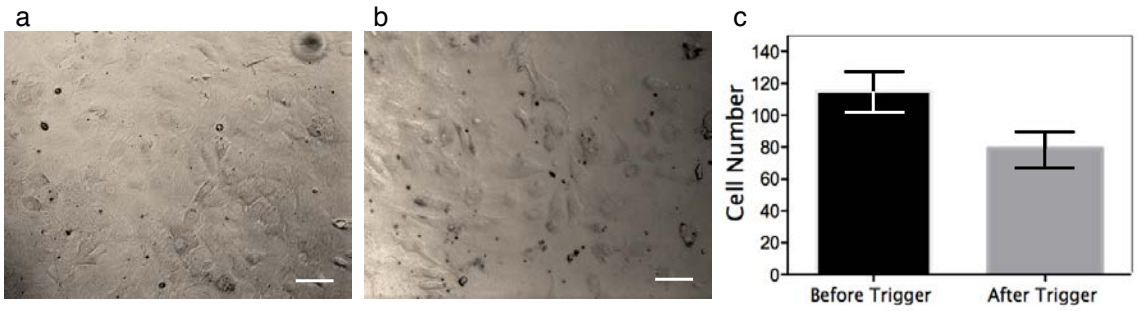

Figure SI 14: Phase contrast images (a) before (a) and (b) after three times repeated electronic stimulation; Cell were counted before and after electronic stimulation using ImageJ. (c) Statistical analysis illustrated that although cell number decreased after stimulation, however, this reduction was not significant. Scale bar is 100μm.

Publications

1. Amir Hossein Sadeghi, Su Ryon Shin, Janine C. Deddens, Giuseppe Fratta, Serena Mandla, Iman K. Yazdi, Gyan Prakash, Silvia Antona, Danilo Demarchi, Marc Buijsrogge, Joost P.G. Sluijter, Jesper Hjortnaes, Ali Khademhosseini*, Engineered 3D Cardiac Fibrotic Tissue to Study Fibrotic Remodeling, Advanced Healthcare Materials, 2017, 6, 1601434

2. Shahid M. Naseer, Amir Manbachi, Yuan Gao, Philipp Walch, Jonathan M. Cooper, Ali Khademhosseini*, Su Ryon Shin*, Surface acoustic waves induced micropatterning of cells in gelatin methacryloyl (GelMA) hydrogels, Biofabrication, 9, 2017, 015020

3. Kai Zhu, Su Ryon Shin*, Tim van Kempen, Yi-Chen Li, Vidhya Ponraj, Amir Nasajpour, Serena Mandla, Ning Hu, Xiao Liu, Jeroen Leijten, Yi-Dong Lin, Mohammad Asif Hussain, Yu Shrike Zhang, Ali Tamayol, Ali Khademhosseini, Gold Nanocomposite Bioink for Printing 3D Cardiac Constructs, Advanced Functional Materials, 2017, 27, 1605352

4. Su Ryon Shin*, Bianca Migliori, Beatrice Miccoli, Yi-Chen Li, Pooria Mostafalu, Jungmok Seo,
Serena Mandla, Alessandro Enrico, Silvia Antonia, Ram Sabarish, Ting Zheng, Pirrami Lorenzo, Kaizhen Zhang, Yu Shrike Zhang, Kai-tak Wan, Demarchi Danilo, Mehmet R. Dokmeci, Ali Khademhosseini*, Electrically Driven Microengineered Bio-inspired Soft Robots, Advanced Materials, under revision

5. Compact Micellization: A Strategy for Ultrahigh T1 Magnetic Resonance Contrast with Gadolinium-Based Nanocrystals, Noah J.J Johnson, Sha He, Viet Anh Nguyen Huu, and Adah Almutairi*, ACS Nano 2016, 10, 8299-8307

6. Simultaneous Enhancement of Photoluminescence, MRI Relaxivity, and CT Contrast by Tuning the Interfacial Layer of Lanthanide Heteroepitaxial Nanoparticles, Sha He, Noah J. J.

Johnson, Viet Anh Nguyen Huu, Esther Cory, Yuran Huang, Robert L. Sah, Jesse V. Jokerst, and Adah Almutairi*, Nano Lett., 2017, 17 (8), pp 4873–4880

7. X. Strakosas, J. Selberg, Z. Hemmatian, and M. Rolandi*, Taking electrons out of bioelectronics: from bioprotonic transistors to ion channels Advanced Science (2017)

8. Z. Hemmatian, E. Jalilian, S. Lee, X. Strakosas, A. Khademhosseini, A. Almutairi, * S. Shin, * M. Rolandi *, Delivery of Cargo with a Bioelectronic Trigger**,** *ACS Appl. Mater. Interfaces* , *10*, 21782 (**2018)**.

9. X Strakosas, J Selberg, X Zhang, N Christie, PH Hsu, A Almutairi, M. Rolandi, A Bioelectronic Platform Modulates pH in Biologically Relevant Conditions, Advanced Science, 1800935 (2018).

Personnel

Marco Rolandi (PI)	8.3%
Ali Khademhosseini (co-PI)	6%
Adah Almutairi (co-PI)	10%
Xenofon Strakosas (postdoc)	80%
Zahra Hemmatian (postdoc)	70%
Mehmet R. Dokmeci (instructor)	5%
Su Ryon Shin (instructor)	5%
Parisa Pour Shahid Saeed Abadi (postdoc)	100%
Amir Nasajpour (postdoc)	100%
Amy Moore- Staff-	18.33%
Peng-Hao Hsu- graduate student	1.33%
Sangeun Lee- graduate student	16.66%
Viet Anh Nguyen Huu- Graduate student	15%
Jason Olejniczak- Graduate Student	18.88%